



Title	The Influence of Force Level and Motor Unit Coherence on Nonlinear Surface EMG Features Examined Using Model Simulation
Authors(s)	McManus, Lara M., Botelho, Diego Pereira, Flood, Matthew W., Lowery, Madeleine M.
Publication date	2019-07-27
Publication information	McManus, Lara M., Diego Pereira Botelho, Matthew W. Flood, and Madeleine M. Lowery. "The Influence of Force Level and Motor Unit Coherence on Nonlinear Surface EMG Features Examined Using Model Simulation." IEEE, July 27, 2019. https://doi.org/10.1109/embc.2019.8857299 .
Conference details	The 41st International Engineering in Medicine and Biology Conference, Berlin, Germany, 23-27 July 2019
Publisher	IEEE
Item record/more information	http://hdl.handle.net/10197/11283
Publisher's statement	© 2019 IEEE. Personal use of this material is permitted. Permission from IEEE must be obtained for all other uses, in any current or future media, including reprinting/republishing this material for advertising or promotional purposes, creating new collective works, for resale or redistribution to servers or lists, or reuse of any copyrighted component of this work in other works.
Publisher's version (DOI)	10.1109/embc.2019.8857299

Downloaded 2026-05-01 23:40:38

The UCD community has made this article openly available. Please share how this access benefits you. Your story matters! (@ucd_oa)



© Some rights reserved. For more information

1 **The Influence of Force Level and Motor Unit Coherence on Nonlinear**
2 **Surface EMG Features Examined Using Model Simulation**

3 Author List: Diego Pereira Botelho, Matthew W. Flood, and Madeleine M. Lowery

4 Corresponding Author: Dr Lara McManus

5 School of Electrical and Electronic Engineering,

6 University College Dublin, Belfield, Dublin 4, Ireland

7 lara.mc-manus@ucdconnect.ie

8 **Affiliations:** L. M. McManus, Diego Pereira Botelho, Matthew W. Flood, and M. M. Lowery are
9 with the School of Electrical and Electronic Engineering, University College Dublin, Ireland.
10 (e-mail: lara.mc-manus@ucdconnect.ie, madeleine.lowery@ucd.ie).

11 **Link to Published Manuscript, DOI:** [10.1109/EMBC.2019.8857299](https://doi.org/10.1109/EMBC.2019.8857299)

12 <https://ieeexplore.ieee.org/document/8857299>

13 **Details of Funding:** Research supported by the European Research Council: ERC-2014-CoG-
14 646923_DBSSModel.

15 © 2019 IEEE. Personal use of this material is permitted. Permission from IEEE must be
16 obtained for all other uses, in any current or future media, including reprinting/republishing this
17 material for advertising or promotional purposes, creating new collective works, for resale or
18 redistribution to servers or lists, or reuse of any copyrighted component of this work in other
19 works.

20 **Abstract**

21 Nonlinear features extracted from surface EMG signals have been previously used to infer
22 information on coherent or synchronous activity in the underlying motor unit discharges.
23 However, it has not yet been assessed how these features are affected by the density of the
24 surface EMG signal, and whether changes in the level of muscle activation can influence the
25 effective detection of correlated motor unit firing. To examine this, a motoneuron pool model
26 receiving a beta-band modulated cortical input was used to generate correlated motor unit firing
27 trains. These firing trains were convolved with motor unit action potentials generated from an
28 anatomically accurate electrophysiological model of the first dorsal interosseous muscle. The
29 sample entropy (SampEn) and percentage determinism (%DET) of recurrence quantification
30 analysis were calculated from the composite surface EMG signals, for signals comprised of both
31 correlated and uncorrelated motor unit firing trains. The results show that although both
32 SampEn and %DET are influenced by motor unit coherence, they are differentially affected by
33 muscle activation and motor unit distribution. The results also suggest that sample entropy may
34 provide a more accurate assessment of the underlying motor unit coherence than percentage
35 determinism, as it is less sensitive to factors unrelated to motor unit synchrony.

36 **Introduction**

37 During steady muscle contractions, motor unit discharges are not completely independent, and
38 their firing trains tend to be weakly coupled across a range of frequencies. Motor unit
39 synchrony, or coherence, is widely believed to reflect functional connectivity between the
40 motoneuron pool and oscillatory cortical activity (Baker et al. 2003; Conway et al. 1995).
41 Changes in corticomuscular, intermuscular and motor unit coherence, particularly within the
42 beta frequency range (15-35Hz), have previously been used to investigate changes in
43 connectivity during neuromuscular fatigue and in disease states (McManus et al. 2016; Norton
44 and Gorassini 2006). Traditionally, motor unit coherence was calculated between pairs of units
45 recorded intramuscularly (Kilner et al. 2002). More recently, composite spike trains have been
46 used to generate enhanced coherence estimates, with each composite train consisting of a
47 number of simultaneously active motor units recorded with surface EMG decomposition (Farina
48 et al. 2014; McManus et al. 2016). Estimation of intramuscular coherence from motor unit firing
49 times provides a high degree of accuracy, however, it requires carefully controlled experimental
50 conditions. To allow more experimental flexibility and facilitate recording of motor unit
51 coherence outside of strict laboratory conditions, several studies have explored alternative
52 features that may provide an assessment of synchrony which can be applied to the surface EMG
53 interference signal (Farina et al. 2002; Holtermann et al. 2009).

54 Nonlinear features of surface EMG signal complexity and deterministic structure can provide a
55 measure of the structure or synchrony in the underlying motor unit activity. Sample entropy
56 (SampEn) and percentage determinism (%DET) of recurrence quantification analysis plots are
57 two such measures that have been shown to capture differences in the surface EMG signal
58 structure under conditions where normal motor unit synchronization is enhanced, including
59 during muscle fatigue (Cashaback et al. 2013; Farina et al. 2002; Mesin et al. 2009; Webber et
60 al. 1995) and in Parkinson's disease (Fattorini et al. 2005; Flood et al. 2019; Meigal et al. 2009).
61 However, these nonlinear features exhibit large intra-subject variability (Flood et al. 2019), and
62 previous studies have suggested that they may be sensitive to factors unrelated to synchrony,
63 including muscle fiber conduction velocity and changes in muscle contraction force (Cashaback
64 et al. 2013; Del Santo et al. 2007; Farina et al. 2002; Istenič et al. 2010; Meigal et al. 2009).
65 Higher levels of muscle activation produce denser surface EMG signals, as additional motor
66 units are recruited, and the firing rates of active units are increased (McManus et al. 2015).
67 Thus, in order to implement SampEn and %DET measures effectively, it is necessary to
68 distinguish how they are affected by alterations in surface EMG density at higher muscle
69 activation levels, in addition to intra-subject differences in physiology (e.g. muscle size, motor
70 unit distribution). The aim of the present study was to investigate how increases in motor unit
71 recruitment and firing rate modulation with increasing muscle activation influence the
72 sensitivity of SampEn and %DET to changes in the underlying motor unit coherence.

73

74 **Methods**

75

76 A model of the motoneuron pool receiving a branched, beta-band modulated cortical input was
77 used to simulate motor unit firing times for 10%, 20%, 30% and 40% of the maximum
78 voluntary contraction (MVC). Motoneuron firing times were convolved with motor unit action
79 potentials, generated from an anatomically accurate electrophysiological model of the first
80 dorsal interosseous (FDI) muscle and the action potential trains were summed to generate four
81 surface EMG channels. The sample entropy and percentage determinism of the surface EMG
82 signals were then calculated for different motor unit distributions, densities, and beta-band
83 modulation strengths.

84 *Motoneuron Model*

85 The model of the motoneuron pool was based on the model described in (Lowery and Erim
86 2005) and was comprised of 100 motoneurons, simulated using a single compartment threshold-
87 crossing model (Powers 1993). In Lowery and Erim (2005) each motoneuron received an
88 independent and common input, comprised respectively of an activation current and a beta-band
89 modulated or oscillatory current. In the present study a more physiologically realistic
90 implementation of the cortical input was used. The correlated common input signal was chosen
91 to generate motor unit coherence spectra qualitatively similar to those recorded experimentally
92 (McManus et al. 2016). First, a beta-band modulated signal was created by summing two band-
93 pass filtered random Gaussian signals, filtered using 4th order Butterworth filters between 12-18
94 Hz and 27-33 Hz, respectively. This beta-band modulated signal was then used as a common
95 input to an integrate and fire encoder, as described in (Halliday 1998), in order to generate 2000
96 weakly correlated spike trains (“corticomotoneuronal (CM) neurons”, Fig. 1). Each motoneuron
97 (MN) received input from 100 of these colored spike trains, with approximately 15% of the
98 signals shared between motoneurons. Each motoneuron also received two independent
99 asynchronous inputs, one excitatory and one inhibitory. Motoneuron input currents were
100 adjusted to produce motor unit activation patterns comparable to those recorded experimentally
101 (McManus et al. 2016; Seki and Narusawa 1996). The force produced by each motor unit, based
102 on the Fuglevand model (Fuglevand et al. 1993), was summed, and the total force generated
103 was continuously compared to a target force (10%, 20%, 30% and 40% MVC) and adjusted
104 based on the difference between the two. To quantify the level of coherent activity in the
105 motoneuron pool, the magnitude squared coherence estimate was obtained from composite
106 spike trains, generated with 40 randomly chosen motor units from the model (McManus et al.
107 2016).

108

109 **Figure 1**110 *Motoneuron Model*

111 The motoneuron pool model was coupled to a model of the FDI muscle based on that described
112 in (Pereira Botelho et al. 2017). Information on anatomically accurate muscle fiber architecture
113 in the FDI muscle during index finger abduction was incorporated into this model, with fiber
114 orientation and curvature derived from diffusion tensor imaging. Physiologically realistic
115 extracellular action potential waveform shapes were generated for the motor unit population
116 using an anatomically accurate finite element model of the hand. This finite element model
117 computed the effect of geometrical and electrical tissue properties on the MUAP shapes and
118 incorporated FDI muscle anisotropy. The electrode used in simulations consisted of five point
119 electrodes located at the corners and center of a 5×5 mm square, based on the electrode used in
120 previous experimental studies (McManus et al. 2015). Pairwise differentiation yielded four
121 action potential representations for each motor unit. Motor unit action potential distributions
122 were generated for the FDI muscle during abduction ($N = 18$). The MUAPs were then
123 convolved with 60 randomly chosen firing trains from the motoneuron model and summed to
124 yield four channels of surface EMG signals. This process was performed for firing trains
125 receiving 1) a weakly beta-band modulated input and 2) no synchronous input.

126 *Nonlinear Measures*

127 Before analysis, the surface EMG signal was lowpass filtered and downsampled to 1kHz.
128 Recurrence quantification analysis was performed on 7 non-overlapping 1.5 s segments of the
129 surface EMG signal during the periods of constant force production in each trial. The
130 parameters selected to calculate the %DET of the recurrence plots were chosen to effectively
131 capture the dynamics of motor unit firing patterns (i.e. time delay = 1, embedding dimension =
132 15 [typical MUAP duration ~ 15 ms], minimum diagonal line = 10 and radius = 20% maximum
133 distance) (Flood et al. 2019; Marwan et al. 2007). The median value over all channels and
134 segments was used as the representative value for %DET. The surface EMG signals were also
135 assessed using SampEn, which is a measure of signal complexity and regularity that has been
136 derived specifically for physiological time-series signals (Richman and Moorman 2000). The
137 SampEn during the constant force trials was calculated over three 7 s windows with an overlap
138 of 4.5 s. The tolerance r for the SampEn calculation was given by 0.2 times the median absolute
139 deviation of the surface EMG signal segment. The embedding dimension was empirically set to
140 3 and the median value over all windows and channels in the 3rd dimension was used as the

141 representative value for SampEn. Full details of the parameters and equations used to calculate
142 %DET and SampEn are provided in (Flood et al. 2019).

143 *Statistics*

144 The influence of both the force level of the muscle contraction (Force) and the underlying beta-
145 band motor unit activity (Beta) were investigated with a linear mixed effects model with
146 maximum likelihood fit using the lme4 library in the software R (Bates et al. 2011). Force and
147 level of beta modulation (ON or OFF) were entered as fixed effects in the model and motor unit
148 distribution was included as a random effect. A random intercept chosen for each motor unit
149 distribution to account for baseline differences in motor unit physiology that could account for
150 some of the variance in SampEn and %DET. The intra-class correlation coefficient (ICC) was
151 also calculated to report the proportion of variance in the nonlinear features that could be
152 explained by the grouping structure (i.e. variability due to differences in the motor unit
153 distribution).

154 **Results**

155 Surface EMG signals were generated from 10%-40% MVC, using motor unit firing trains that
156 were uncorrelated, Fig. 2 (A) & (B), or moderately correlated in the beta-band range, Fig. 2 (C)
157 & (D). The SampEn and %DET values for both uncorrelated and correlated motor unit firing
158 trains are shown for each simulated force level in Fig. 3. The relative effect of contraction force
159 and correlation in the motor unit discharges on the nonlinear measures is summarized in Table
160 1. The ICC for SampEn was 0.04, lower than the 0.31 observed for %DET.

161

162 **Figure 2**

163 **Figure 3**

164 **Table 1**

165

166 **Discussion**

167 The present study demonstrates that surface EMG sample entropy and percentage determinism
168 can be used to provide information on correlated or synchronous motor unit activity, but that
169 future studies should consider the level of muscle activation as an additional factor that could
170 significantly influence these measures. The results show for the first time that SampEn and
171 %DET are disparately affected by properties of the surface EMG signal unrelated to motor unit
172 synchrony. The higher ICC value reported for %DET suggests that this measure is more
173 sensitive to motor unit distribution representative of intra-subject differences in motor unit
174 physiology. If few active motor units are distributed within the detection volume of the
175 recording electrode, this could result in a sparse EMG signal with action potentials from a small
176 number of units dominating the EMG signal, particularly at lower force contractions. These
177 sparse EMG signals are likely to affect the accuracy at which recurring states are identified. A
178 recurrence is marked each time the phase space trajectory returns to a location in phase space
179 that it has visited before, within a designated radius. In the present study, the radius was chosen
180 as a percentage of the maximum inter-state distance, which at low forces could effectively be
181 the action potential amplitudes of a small number of motor units. Thus, random fluctuations in
182 the EMG signal voltage that do not contain any information on motor unit activity may be more
183 likely to fall within the radius and be marked as a recurrence. This could also explain why
184 %DET measures were more sensitive than SampEn to increases in motor unit recruitment and
185 firing rate modulation with increasing abduction force, Table 1. As the density of the surface
186 EMG signal is increased, the maximum inter-state distance becomes more representative of the
187 mean amplitude of the signal, and recurrence identification is likely to be more accurate.
188 Accordingly, %DET increased significantly in the presence of beta-band motor unit coherence
189 at 30% and 40%MVC, Fig. 3 (B).

190 Though SampEn was also influenced by the level of muscle activation, the presence of coherent
191 beta-band activity in the underlying motor unit discharges had a greater effect on the SampEn
192 value, Table 1. Beta-band activity was effectively detected at all force levels, Fig. 3 (A). The
193 results suggest that SampEn should be preferred over %DET to detect changes in motor unit
194 coherence in conditions where changes in coherent activity could be masked by alterations in
195 the composition or density of the surface EMG signals (i.e. at different muscle forces or when
196 comparing EMG between healthy and disease states). Collectively, the results highlight that the
197 utility of SampEn and %DET measures lies in detecting changes or differences in motor unit
198 coherence between conditions or subject groups, and that an individual SampEn/%DET value
199 should not be used in isolation to infer information on the absolute strength of correlated motor
200 unit activity.

201 The results presented have examined surface EMG signals simulated for an electrode array with
202 small electrode surface area and inter-electrode distance in the first dorsal interosseous muscle.
203 However, the relative sensitivity of both nonlinear features to muscle activation and correlated
204 motor unit activity could be influenced by the muscle geometry and electrode configuration.
205 Further work is needed to investigate whether the results of the present study would change for
206 other electrode configurations. A bipolar electrode with larger inter-electrode distance would
207 have a larger detection volume, with denser surface EMG signals containing information on the
208 activity of a larger motor unit sample. EMG signals simulated for other muscles could also
209 exhibit distinct trends. For example, larger limb muscles have fewer cortical connections than
210 the muscles of the hand, and the correlation between motor unit firing trains from these muscles
211 could be weaker as a result. Higher levels of subcutaneous fat would also influence the structure
212 of the surface EMG signal, as surface-detected action potentials would be longer in duration due
213 to the spatial low pass filtering effect of the tissue (Lowery et al. 2002). Future work could also
214 explore whether alternative methods of calculating the radius are more accurate at detecting
215 recurrences, for example the fixed amount of nearest neighbors method (Marwan et al. 2007).
216 Finally, the results highlight the need for further simulation work to elucidate how each of the
217 nonlinear features could be optimized to expressly detect changes in motor unit coherence.

218

219

220 **References**

- 221 **Baker SN, Pinches EM, and Lemon RN.** Synchronization in monkey motor cortex during a
 222 precision grip task. II. Effect of oscillatory activity on corticospinal output. *Journal of*
 223 *neurophysiology* 89: 1941-1953, 2003.
- 224 **Bates D, Maechler M, and Bolker B.** lme4: linear mixed-effects models using Eigen and
 225 Eigen. R package version 0.999375-42. 2011. *Google Scholar* 2011.
- 226 **Cashaback JG, Cluff T, and Potvin JR.** Muscle fatigue and contraction intensity modulates the
 227 complexity of surface electromyography. *Journal of Electromyography and Kinesiology* 23: 78-
 228 83, 2013.
- 229 **Conway B, Halliday D, Farmer S, Shahani U, Maas P, Weir A, and Rosenberg J.**
 230 Synchronization between motor cortex and spinal motoneuronal pool during the performance
 231 of a maintained motor task in man. *The Journal of physiology* 489: 917-924, 1995.
- 232 **Del Santo F, Gelli F, Ginanneschi F, Popa T, and Rossi A.** Relation between isometric muscle
 233 force and surface EMG in intrinsic hand muscles as function of the arm geometry. *Brain*
 234 *research* 1163: 79-85, 2007.
- 235 **Farina D, Fattorini L, Felici F, and Filligoi G.** Nonlinear surface EMG analysis to detect changes
 236 of motor unit conduction velocity and synchronization. *Journal of Applied Physiology* 93: 1753-
 237 1763, 2002.
- 238 **Farina D, Negro F, and Dideriksen JL.** The effective neural drive to muscles is the common
 239 synaptic input to motor neurons. *The Journal of physiology* 592: 3427-3441, 2014.
- 240 **Fattorini L, Felici F, Filligoi G, Trallesi M, and Farina D.** Influence of high motor unit
 241 synchronization levels on non-linear and spectral variables of the surface EMG. *Journal of*
 242 *neuroscience methods* 143: 133-139, 2005.
- 243 **Flood M, Jensen B, Mallin A, and Lowery M.** Increased Emg Intermuscular Coherence and
 244 Reduced Signal Complexity in Parkinson's Disease. *Clinical neurophysiology* 2019.
- 245 **Fuglevand AJ, Winter DA, and Patla AE.** Models of recruitment and rate coding organization in
 246 motor-unit pools. *Journal of neurophysiology* 70: 2470-2488, 1993.
- 247 **Halliday D.** Generation and characterization of correlated spike trains. *Computers in biology*
 248 *and medicine* 28: 143-152, 1998.
- 249 **Holtermann A, Grönlund C, Karlsson JS, and Roeleveld K.** Motor unit synchronization during
 250 fatigue: described with a novel sEMG method based on large motor unit samples. *Journal of*
 251 *Electromyography and Kinesiology* 19: 232-241, 2009.
- 252 **Istenič R, Kaplanis PA, Pattichis CS, and Zazula D.** Multiscale entropy-based approach to
 253 automated surface EMG classification of neuromuscular disorders. *Medical & biological*
 254 *engineering & computing* 48: 773-781, 2010.
- 255 **Kilner J, Alonso-Alonso M, Fisher R, and Lemon R.** Modulation of synchrony between single
 256 motor units during precision grip tasks in humans. *The Journal of physiology* 541: 937-948,
 257 2002.
- 258 **Lowery MM, and Erim Z.** A simulation study to examine the effect of common motoneuron
 259 inputs on correlated patterns of motor unit discharge. *Journal of computational neuroscience*
 260 19: 107-124, 2005.
- 261 **Lowery MM, Stoykov NS, Taflove A, and Kuiken T.** A multiple-layer finite-element model of
 262 the surface EMG signal. *Biomedical Engineering, IEEE Transactions on* 49: 446-454, 2002.
- 263 **Marwan N, Romano MC, Thiel M, and Kurths J.** Recurrence plots for the analysis of complex
 264 systems. *Physics reports* 438: 237-329, 2007.
- 265 **McManus L, Hu X, Rymer WZ, Lowery MM, and Suresh NL.** Changes in motor unit behavior
 266 following isometric fatigue of the first dorsal interosseous muscle. *Journal of neurophysiology*
 267 113: 3186-3196, 2015.

- 268 **McManus L, Hu X, Rymer WZ, Suresh NL, and Lowery MM.** Muscle fatigue increases beta-
269 band coherence between the firing times of simultaneously active motor units in the first
270 dorsal interosseous muscle. *Journal of neurophysiology* 115: 2830-2839, 2016.
- 271 **Meigal AI, Rissanen S, Tarvainen M, Karjalainen P, Iudina-Vassel I, Airaksinen O, and**
272 **Kankaanpää M.** Novel parameters of surface EMG in patients with Parkinson's disease and
273 healthy young and old controls. *Journal of Electromyography and Kinesiology* 19: e206-e213,
274 2009.
- 275 **Mesin L, Cescon C, Gazzoni M, Merletti R, and Rainoldi A.** A bi-dimensional index for the
276 selective assessment of myoelectric manifestations of peripheral and central muscle fatigue.
277 *Journal of Electromyography and Kinesiology* 19: 851-863, 2009.
- 278 **Norton JA, and Gorassini MA.** Changes in cortically related intermuscular coherence
279 accompanying improvements in locomotor skills in incomplete spinal cord injury. *Journal of*
280 *neurophysiology* 95: 2580-2589, 2006.
- 281 **Pereira Botelho D, Colgan N, Fagan A, Curran K, and Lowery M.** Influence of muscle
282 architecture on the sEMG signal of the first dorsal interosseous muscle: A subject-specific
283 model based on diffusion tensor imaging. *Program No 41211 2017 Neuroscience Meeting*
284 *Planner Washington, DC: Society for Neuroscience, 2017 Online* 2017.
- 285 **Powers RK.** A variable-threshold motoneuron model that incorporates time-and voltage-
286 dependent potassium and calcium conductances. *Journal of neurophysiology* 70: 246-262,
287 1993.
- 288 **Richman JS, and Moorman JR.** Physiological time-series analysis using approximate entropy
289 and sample entropy. *American Journal of Physiology-Heart and Circulatory Physiology* 278:
290 H2039-H2049, 2000.
- 291 **Seki K, and Narusawa M.** Firing rate modulation of human motor units in different muscles
292 during isometric contraction with various forces. *Brain research* 719: 1-7, 1996.
- 293 **Webber C, Schmidt M, and Walsh J.** Influence of isometric loading on biceps EMG dynamics as
294 assessed by linear and nonlinear tools. *Journal of Applied Physiology* 78: 814-822, 1995.
- 295

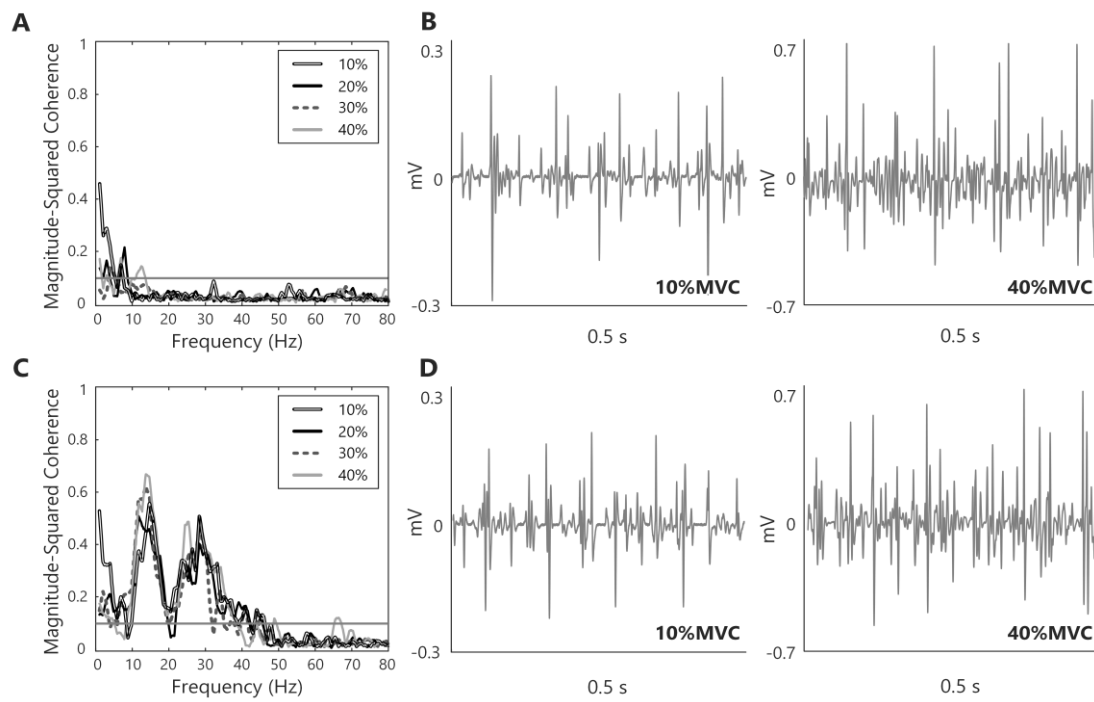


Figure 2. Motor unit coherence when there was (A) no correlated input to the motoneuron and (C) correlation in the beta-band range, and the corresponding surface EMG signals, (B) & (D) respectively, at 10%MVC and 20%MVC.

297

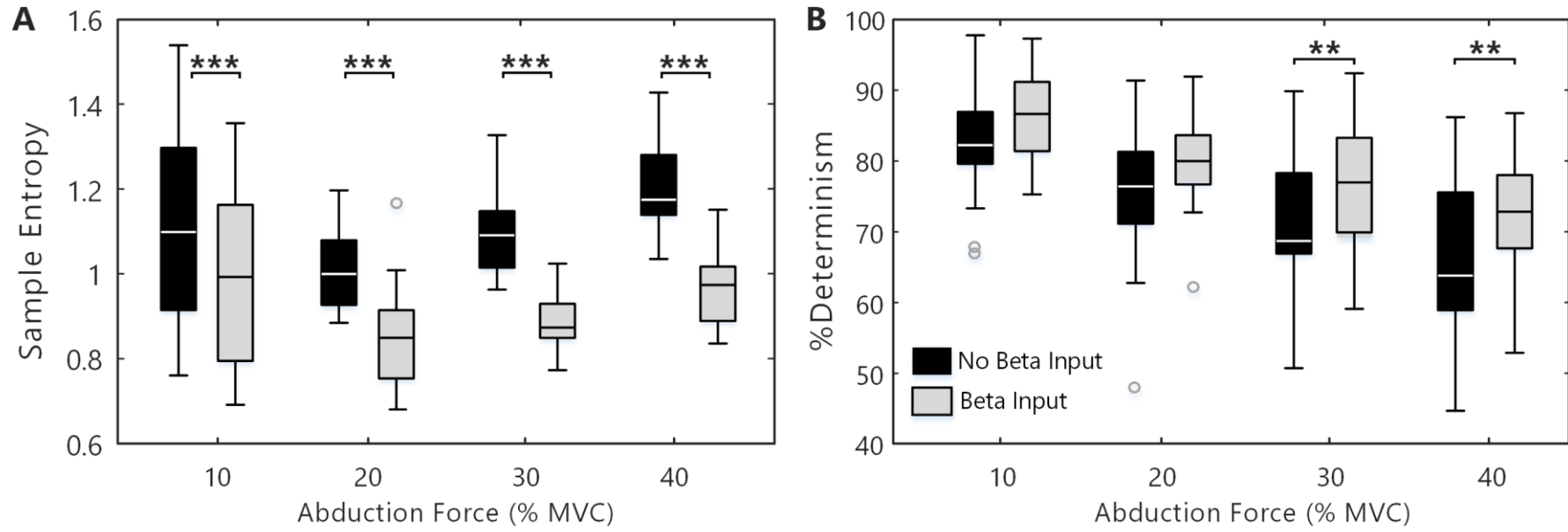


Figure 3. (A) SampEn and (B) %DET at each force level with either no correlated input to the motoneuron or beta-band correlation, **p<.01, ***p<.001.

298

299

300

TABLE I. MIXED MODEL ANOVA RESULTS

A	Sample Entropy			
<i>Model Term</i>	<i>df 1/2</i>	<i>F-Stat</i>	<i>p-value</i>	<i>Partial R²</i>
Force	3/122	8.4	<.001	0.1
Beta	1/122	16.1	<.001	0.26

301

B	% Determinism			
<i>Model Term</i>	<i>df 1/2</i>	<i>F-Stat</i>	<i>p-value</i>	<i>Partial R²</i>
Force	3/122	26.9	<.001	0.62
Beta	1/122	16.6	<.001	0.05

302

303 Table 1. Mixed model ANOVA results using the Kenward-Roger approximation for degrees of freedom investigating the effect of abduction force
 304 (Force) and correlated beta-band input (Beta) on (A) sample entropy and (B) percentage determinism.

305